"THE PERFORMANCE AND MODELLING OF 8 PHOTOVOLTAIC MATERIALS UNDER VARIABLE LIGHT INTENSITY AND SPECTRA"

J. F. RANDALL, J. JACOT
LPM, IPR, STI, EPFL, CH-1015 Lausanne, Switzerland
Telephone: ++ 41 21 693 5945 Fax: ++ 41 21 693 3891 E-mail: Julian.Randall@epfl.ch

ABSTRACT

Solar cell comparison is generally based on a theoretical maximum terrestrial intensity and spectra (of 1 sun) at 25°C perpendicular to the cell plane. In practice, no solar cell experiences such conditions, yet few alternative bases for comparison exist. Those that do suffer drawbacks, such as energy payback studies; the latter are typically handicapped by the natural variations of outdoor temperature and spectrum. Spectrum in particular is difficult to correct for.
Our interest in this paper is to explore the correct design of indoor Photovoltaic (IPV) products. Given that the indoors, when compared with the outdoors, are characterised by much lower radiant energy intensities, more spectra and less temperature variation, it is clear that complete comparison data for indoor conditions is not freely available.
This paper presents experimental results for 21 different solar cells representing 8 different Photovoltaic material technologies. These are reproducibly electrically characterised under a laboratory based simulated AM1.5 (1 sun; solar spectrum at 1000W/m2 intensity) using the same spectrum and temperature across the four orders of magnitude below 1 sun (to the 0.1 – 1W/m2 decade). Their electrical performance was also measured under an artificial light source (fluorescent tube) across a number of points in the 1-10W/m2 decade. The results presented are compared with a phenomenologically based model. Its successful validation suggests that it could be applied for electrical yield predictions across the IPV range of radiant energy intensities.

INTRODUCTION

The inexorable growth in low power micro-electronic devices such as sensors and MEMS is an opportunity for increasing the use of PV (Photovoltaics) especially for indoor applications. Cells and modules can be used to either partially or completely source their charge requirements. Indoor consumer PV represented over 3% of 1997 world production, so extrapolating to the present global PV production of around 350MW_p, the present indoor consumer segment can be expected to surpass 10MW_p. It is of note that the 1 sun efficiency reference of these statistics is misleading for indoor products, as electrical efficiency is much less important indoors. This is because the end-user decision to purchase an indoor PV (IPV) product is not related to the solar cell electrical efficiency but rather to such benefits as reduced reliance on batteries ("plug and forget") and increased reliability i.e. a correctly designed and used IPV system can run longer without user intervention. From an environmental responsibility perspective, extending battery life is also laudable.
This paper forms part of a wider project to examine how to extend IPV use beyond the solar calculators and watches to which we are already accustomed. Whilst data is available to the IPV designer, such as PV materials available, cost, colour, surface areas, 1 sun voltage/current and so on, there remain areas of missing and yet salient information. One of these areas is comparable electrical performance at the light intensities and spectra typical of the indoor environment (<10W/m2 at >1m from artificial light source or <100W/m2 at >1m from window). Another is a suitable model to describe such performance.
Using solar cells indoors is both different from outdoors (less variation of temperature, much less intensity {1-10W/m2 range rather than 100-1000W/m2 range outside}, further spectra, variation of performance with intensity) and similar (importance of cell orientation with respect radiant energy source/s, impact of obstacles).

These issues are more easily understood when one considers those who influence the built environment namely the creators (architects and lighting engineers in the case of IPV) and end-users. Architects when designing in practice try to achieve a balance between a number of factors including safety, cost and comfort (light, temperature, aesthetics etc.). Chief among these for IPV needs is the light levels which they attempt to maintain as uniform as possible, although this is rarely possible by daylight alone. The reason for this can be seen in Figure 1, showing typical values of Daylight Factor (DF), which are quite low (a few percent). DF is calculated by the ratio of L_{int}/L_{ext}, where L_{int} and L_{ext} are the light levels in Lux indoors and outdoors respectively. Note the rapid decrease of DF between window and opposite wall to which the human eye adapts imperceptibly.

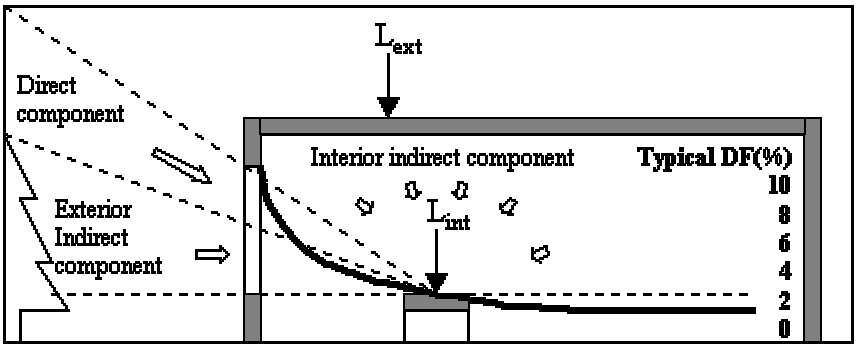

Figure 1: Daylight factor components and typical values

Lighting engineers aim to fulfil a specification from an architect that complements the daylight component, with the aim of providing whatever artificial lighting will be required. Users are a stochastic element in any system that can be modelled. They can have a significant impact on the available light by the fittings and furniture they require as well as their use-pattern, e.g. how they use lighting and blinds.

These 3 groups of actors seek a perceived (or photometric) result, whilst PV collects radiant energy. For this paper, the word "light" is used to describe photometric radiation whilst "radiant energy" (E_{rad}) is used for the wider bandwidth radiation to which solar cells are sensitive. Our experiments measuring E_{rad} indoors have confirmed similar trends to those found for light (or DF) shown in Figure 1.

In order to increase the range of experiments, simulation can be performed with relatively less resources (time, number of sensors, varying less parameters at a time i.e. daylight variation during measurement). The choice of software should be made by prioritising physical accuracy and as such "Radiance"[1] is ideal. The solar cell data presented in this paper when combined with predicted E_{rad} data allow the cumulative charge (Ah) available to be calculated.

Following this section the method used for testing the cells is described (Experimental Procedure) as well as the related findings (Results). In the Model Presentation section, a model will be explained and compared with the results. Other issues of interest are then reviewed in the Discussion.

EXPERIMENTAL PROCEDURE

We sought to characterise the solar cells under indoor conditions, whilst departing as little as possible from Standard Test Conditions (STC) [2]. The current/voltage (I/V) characteristics were taken in the standard way for the 21 samples in Table 1 using a Wacom solar simulator as previously described [3]; the E_{rad} intensity was controlled with one or more wire mesh filters between the E_{rad} source and the sample which at maximum filtration reduced the 1000W/m2 to approximately 0.8W/m2. At each level of intensity, an I/V measurement was made.

Some samples were also tested under a separate artificial E_{rad} source (the fluorescent Philips Ecotone PL-L, 830/4P HF, 40W) over a smaller range of intensities (1-5W/m^2). The intensity from this artificial light source on the solar cell was varied by controlling the distance (>1m) between the source and the solar cell under test.

The indoor environment typically has a smaller temperature range than outdoors, so all experiments were performed at a fixed temperature (22°C +/-3). This contributed to reducing the uncertainty related to varying more than one variable at a time, often found in outdoor comparative testing.

Technological Classification	Supplier or Laboratory Name	Indu. = I Labo = L	Active Area (cm^2)	No. of cells in module
Silicon (crystalline)	BP Solar (via IWS)	I	9.36	1
Silicon (crystalline LGBC)	BP Solar, UK	I	0.90	1
Silicon (crystalline)	Spacecells, Edmund Scientifc, US	I	0.38	1
Silicon (crystalline)	Unknown (via Distributor)	I	10.95	1
Silicon (multicrystalline)	MAIN, TESSAG, D	I	12.47	1
Silicon (multicrystalline)	EFG, TESSAG, D	I	10.25	1
Silicon (multicrystalline)	Unknown (via Distributor)	I	2.88	1
III-V cells (GaAs)	NREL, Golden, CO, US	L	0.25	1
Polycrystalline thin film (CdTe)	Matsushita / Panasonic, J	I	5.80	5
Polycrystalline thin film (CdTe)	Parma University, I	L	0.79	1
Polycrystalline thin film (CIGS)	ZSW, Stuttgart University, D	L	0.46	1
Other (GaInP)	NREL, Golden, CO, US	L	0.25	1
Amorphous Silicon	TESSAG, Putzbrunn, D	I	4.95	5
Amorphous Silicon	Sanyo Electric, Hyogo, J	I	3.71	4
Amorphous Silicon	Solems, Paris, F	I	1.76	3
Amorphous Silicon	VHF Technologies, Le Locle, CH	L	3.36	4
Amorphous Silicon	Sinonar Corporation, Taipei, TW	I	1.26	4
Amorphous Silicon	Millenium, BP Solar, UK	I	1.20	1
Photochemical (Nanocrystalline dye)	Greatcell SA, Yverdon, CH	L	1.00	1
Photochemical (Nanocrystalline dye)	EPFL, IPC2, Lausanne, CH	L	0.9	1
Multijunction cell (GaAs+GaInP tandem)	NREL, Golden, CO, US	L	0.25	1

Table 1: Technologies and sources of the 21 cells tested showing whether the manufacturer was a laboratory or industry, the active area and number of cells in the module of each sample tested [4]

RESULTS

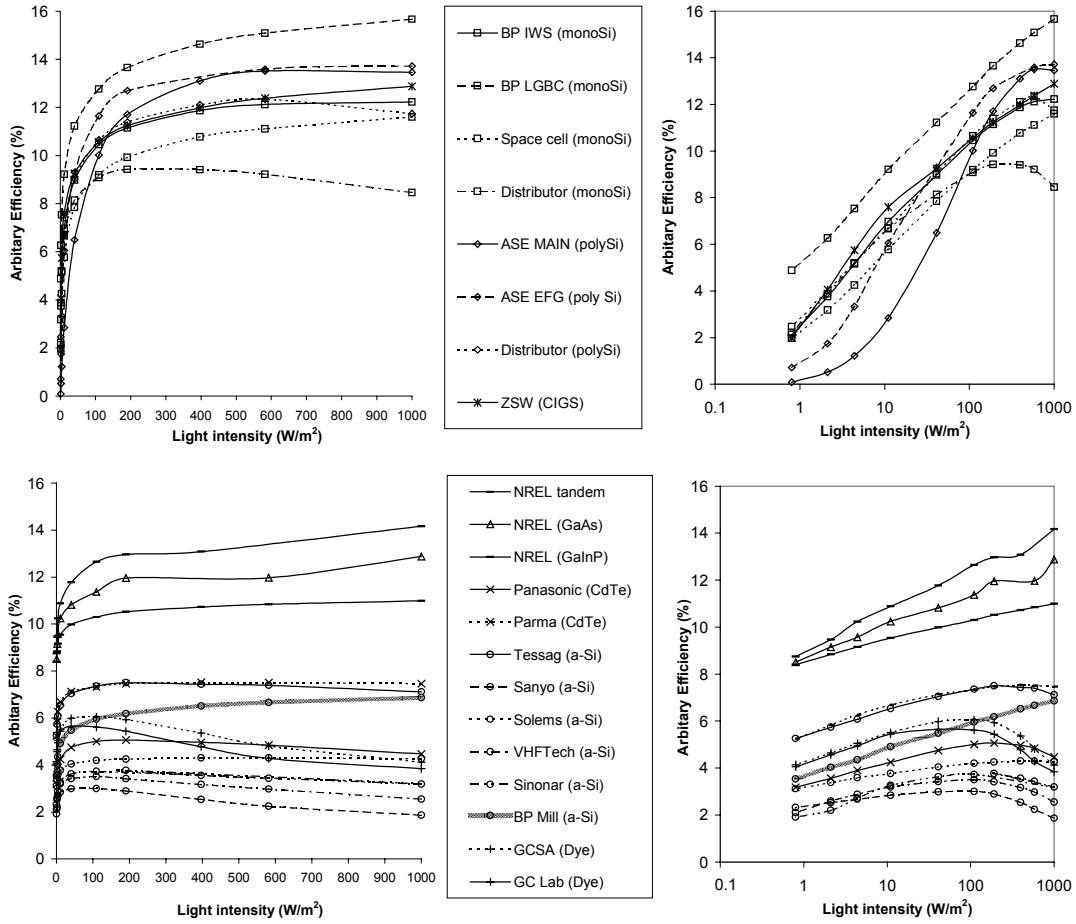

Figure 2: Efficiency of all samples under wire-mesh filtered AM1.5 (1000W/m2) showing the same results against intensity on the base 10 scale (left) and natural logarithm (right). The log scale slope has been used to sort the results between the top and bottom graphs (see phenomenological model).

Samples were accepted for testing on the basis that they were not necessarily designed with the goal of having the highest one sun efficiency possible. It is clear therefore that these results are representative of an average quality cell performance i.e. the quality that a practitioner may encounter. For this reason, the y-axis in Figure 2, 3 and 5 is referred to as "arbitrary efficiency".

Figure 2 (left graphs) shows that solar cell efficiency in the highest intensity decade, 100-1000W/m^2, does not vary appreciably and that the ranking of 1 sun efficiency is almost completely maintained down to 200W/m^2.

For intensities below 100W/m^2 (see Figure 2 right graphs), which are typical of indoor conditions, a much more marked change is found and the ranking by technology is altered when one reaches the lowest intensities so that some of the highest performing cells at 1 sun were the weakest at 1W/m^2.
The graphs in Figure 3 compare the efficiencies under filtered AM1.5 with those found under the fluorescent source for selected samples representing 3 technologies. The fluorescent intensity was measured using a Lux meter and then converted to W/m^2 using the (simplified) relationship:

$$\frac{E_{rad}(Lux)}{120{,}000} = \frac{E_{rad}(W/m^2)}{1{,}000} \qquad (1)$$

or:

$$E_{rad}(W/m^2) = \frac{E_{rad}(Lux)}{120} \qquad (2)$$

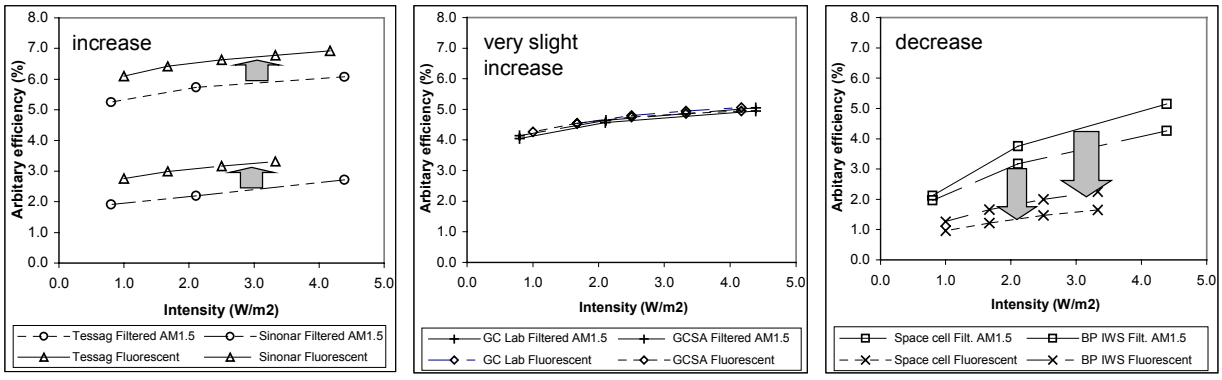

Figure 3: Efficiency difference going from filtered AM1.5 to the fluorescent spectrum for 2 samples of 3 PV technologies: amorphous Silicon single cells (left), dye cell (middle) and crystalline Silicon (right)

MODEL PRESENTATION

Efficiency (η) is calculated as follows:

$$\eta = \frac{FF \times I_{SC} \times V_{OC}}{G} \qquad (3)$$

where FF is Fill Factor, I_{SC} is short circuit current, V_{OC} is open circuit voltage and G is intensity (equal to E_{rad}).

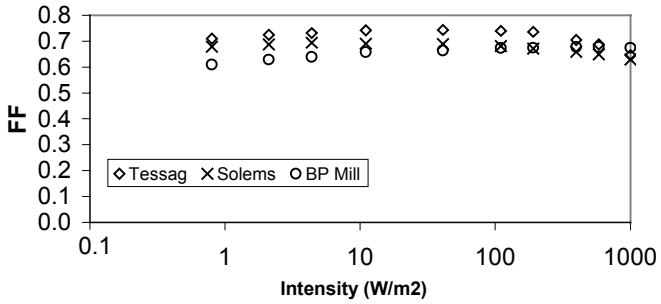

Figure 4: FF with respect to Intensity on base 10 log. scale for selected amorphous Silicon samples

For the samples in Figure 4 it can be seen that FF is approximately constant [5] in the range 1-100W/m^2. Moreover, it also well known that I_{SC} is directly proportional to G; in this case αG is used instead of I_{SC} where α is a constant:

$I_{sc}=\alpha G$ (4)

Given that Voc has the following relationship with I_{SC}:

$$V_{OC} \cong \frac{kT}{q}\ln\left(\frac{I_{SC}}{I_S}\right) \quad (5)\ [6]$$

where I_s is the saturation current and kT/q is the thermal voltage, substituting (4) and (5) into equation (3), we find that:

$$\eta \cong FF \cdot \alpha \cdot \frac{kT}{q}(\ln G + \ln\alpha - \ln I_S) \quad (6)$$

I_S can be found [7] & [8] using the approximate formula:

$$I_S \cong \beta \exp\left(-\frac{E_g}{kT}\right) \quad (7)$$

where E_g is the band gap; assuming β is relatively constant, equation (6) becomes:

$$\eta \cong FF \cdot \alpha \cdot \frac{kT}{q}\left(\ln G + \ln\alpha - \ln\beta + \frac{E_g}{kT}\right) \quad (8)$$

which in the form:

$$\eta = a\ln G + b \quad (9)$$

has:

$$a = FF \cdot \alpha \cdot \frac{kT}{q} \quad (10)$$

and:

$$b = FF \cdot \alpha \cdot \frac{kT}{q}\left(\ln\alpha - \ln\beta + \frac{E_g}{kT}\right) \quad (11)$$

From the right hand graphs of Figure 2, it is clear that the overall trend is a straight line on a logarithmic scale. This is particularly the case in the range 1-100W/m^2 and for the lower right hand graph. In Figure 5 we magnify the efficiency range 1-100W/m^2 and compare it with a line whose equation is of the same form as equation 9. This latter relationship was applied to the data for all samples in the range 0.8-100W/m^2 and the results shown in Table 2 suggest a good fit (average R^2 for all samples of 0.98 [9]).
An ideal cell for IPV use therefore has as low a value for *a* and as high a value for *b* as possible, as displayed by those samples that perform the best in our experiments under indoor light conditions (e.g. Ga compounds).
Also of note, the data in Table 2 is ranked according to *a*. As can be seen, two distinct technological groups are found. Those with a value of *a* greater than 1.4 (left-hand side of Table 2, including mono-crystalline Silicon, polycrystalline Silicon and CIGS) and *a* in the range 0.17 – 0.74 (on the right hand side, amorphous Silicon, CdTe, Gallium compounds and dye cells). These two modes have already been identified [3] and this is the first time that a numerical variable has been associated with them.

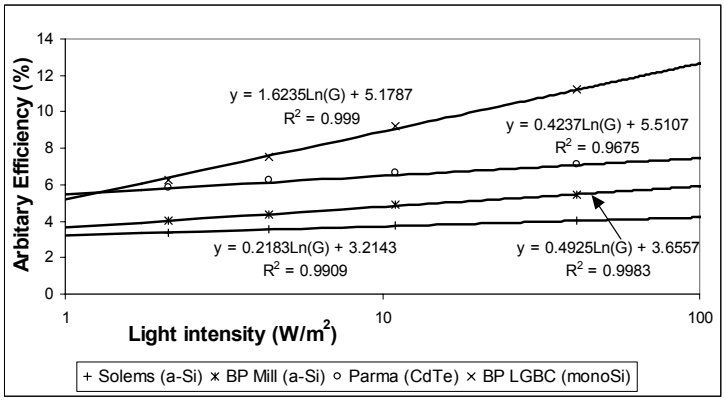

Figure 5: A magnification of the right hand side of Figure 2 for selected samples compared with the fit of equation 9

Technological Classification	Supplier or Laboratory Name	a_{AM}	b_{AM}	R^2
Silicon (multicrystalline)	EFG, TESSAG, D	2.33	0.48	0.99
Silicon (multicrystalline)	MAIN, TESSAG, D	2.05	-0.84	0.92
Polycrystalline thin film (CIGS)	ZSW, Stuttgart University, D	1.73	2.83	0.98
Silicon (crystalline)	BP Solar (via IWS)	1.71	2.58	1.00
Silicon (multicrystalline)	Unknown (via Distributor)	1.67	2.80	1.00
Silicon (crystalline LGBC)	BP Solar, UK	1.62	5.18	1.00
Silicon (crystalline)	Spacecells, Edmund Scientifc, US	1.50	2.16	1.00
Silicon (crystalline)	Unknown (via Distributor)	1.40	2.88	0.99
Nb: a_{AM} and b_{AM} are the values of a and b under AM1.5				
Average R^2 for all 21 samples				0.98

Technological Classification	Supplier or Laboratory Name	a_{AM}	b_{AM}	R^2
Multijunction cell (GaAs+GaInP tandem)	NREL, Golden, CO, US	0.74	9.02	0.99
III-V cells (GaAs)	NREL, Golden, CO, US	0.57	8.72	0.98
Amorphous Silicon	Millenium, BP Solar	0.49	3.66	1.00
Amorphous Silicon	TESSAG, Putzbrunn, D	0.43	5.41	0.99
Polycrystalline thin film (CdTe)	Parma University, I	0.42	5.51	0.97
Photochemical (Nanocrystalline dye)	EPFL, IPC2, Lausanne, CH	0.42	4.25	0.95
Photochemical (Nanocrystalline dye)	Greatcell SA, Yverdon, CH	0.40	4.37	0.96
Amorphous Silicon	Sinonar Corporation, Taipei, TW	0.40	2.06	0.95
Polycrystalline thin film (CdTe)	Matsushita / Panasonic, J	0.38	3.30	1.00
Other (GaInP)	NREL, Golden, CO, US	0.36	8.59	1.00
Amorphous Silicon	VHF Technologies, Le Locle, CH	0.33	2.30	0.96
Amorphous Silicon	Solems, Paris, F	0.22	3.21	0.99
Amorphous Silicon	Sanyo Electric, Hyogo, J	0.17	2.39	0.98

Table 2: The parameters of the phenomenological model (equation 9) over the 1-100W/m^2 range for all samples tested under AM1.5

Technological Classification	Supplier or Laboratory Name	a_F	b_F	R^2
Silicon (crystalline)	BP Solar (via IWS)	0.82	1.26	1.00
Silicon (crystalline)	Spacecells, Edmund Scientifc, US	0.57	0.95	1.00
Nb: a_F and b_F are the values of a and b under the fluorescent source				
Average R^2 for all 6 samples				1.00

Technological Classification	Supplier or Laboratory Name	a_F	b_F	R^2
Amorphous Silicon	Sinonar Corporation, Taipei, TW	0.46	2.76	1.00
Amorphous Silicon	TESSAG, Putzbrunn, D	0.57	6.11	1.00
Photochemical (Nanocrystalline dye)	EPFL, IPC2, Lausanne, CH	0.57	4.26	1.00
Photochemical (Nanocrystalline dye)	Greatcell SA, Yverdon, CH	0.48	4.29	0.99

Table 3: Phenomenological model (equation 9) parameters over the 1-100W/m^2 range for samples tested under the fluorescent source

Technological Classification	Supplier or Laboratory Name	a_F/a_{AM}	b_F/b_{AM}
Silicon (crystalline)	BP Solar (via IWS)	0.48	0.49
Silicon (crystalline)	Spacecells, Edmund Scientifc, US	0.38	0.44

Technological Classification	Supplier or Laboratory Name	a_F/a_{AM}	b_F/b_{AM}
Amorphous Silicon	Sinonar Corporation, Taipei, TW	1.15	1.34
Amorphous Silicon	TESSAG, Putzbrunn, D	1.32	1.13
Photochemical (Nanocrystalline dye)	EPFL, IPC2, Lausanne, CH	1.36	1.00
Photochemical (Nanocrystalline dye)	Greatcell SA, Yverdon, CH	1.18	0.98

Table 4: The ratio of fluorescent parameters (Table 3) to AM1.5 parameters (Table 2)

Table 3 shows the parameters of equation 9 for the results in Figure 3. These are then compared with the values under AM1.5 (Table 2). As can be seen in Table 4, the amorphous Silicon parameters increase by 13-34%. The dye cell samples little change in parameter *b* and an 18-36% increase in parameter *a*. The crystalline Silicon samples parameters decrease from 51-62%. This indicates that the latter samples are more greatly affected by this spectral change than the amorphous and dye cells.

DISCUSSION

The effect of series resistance (R_S) and parallel (shunt) resistance (R_P) on solar cell I/V curves is known [10], see equivalent circuit in Figure 6. At high E_{rad} intensity, R_S reduces FF whilst at low E_{rad}, R_P reduces FF. The "knock-on" effect of R_S and R_P on efficiency can be seen in the gradient of the curves in Figure 2. It can be assumed that for the part of each curve where the gradient is positive, low R_P is the main efficiency deterioration effect (MEDE). Some samples in the intensity decade 100-1000 W/m^2 have a negative gradient that suggests that high R_S is the MEDE. At the intensities between these two effects, where the gradient approaches zero, the efficiency is maximised. For IPV products in particular, knowledge of these efficiency variations can improve product and cell design as well as help to explain variations in performance of ostensibly similar modules.

As a complement to the results, it would be interesting to test further cell samples, especially of those technologies which are not as well represented here (e.g. CIGS) and/or those that performed well at low light levels, such as CdTe and the Gallium compounds. This would allow further scrutiny and improvement of the model presented.

An ideal outcome from the IPV practitioner perspective would be a model based on easily accessible data (such as 1 sun efficiency) which would provide a prediction of cell performance over the full range of intensities tested here. The phenomenological model (equation 8) is valid for only some of the samples across the full range tested, 0.8-1000W/m2, namely Solems, BP Millenium and Tessag. In order to extend the validity, more terms are required to model that part of the efficiency-intensity curve where the gradient becomes negative, i.e. R_S is the MEDE. It is also necessary to investigate the physical meaning of the control parameters *a* (equations 10) and *b* equation (11).

Another area requiring better understanding is the physical mechanism which induces R_p. It has been stated [11] that "the short circuit resistance R_{SC} for lowest illumination levels equals ... the R_P of the device". Taking the R_{SC} for a selection of samples at a low E_{rad} (4.4W/m^2 in this case) the R_P can be estimated. Figure 7 suggests that there is a natural log relationship between R_P and efficiency per technology.

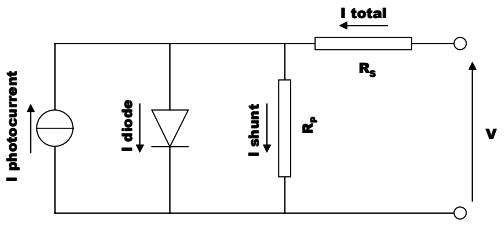

Figure 6: Equivalent circuit of Photovoltaic solar cell or module

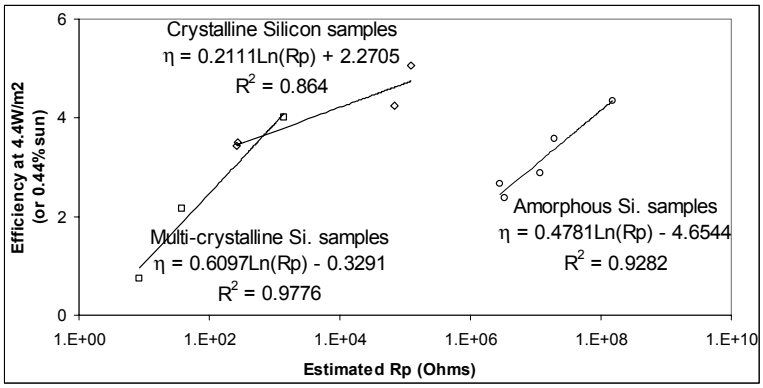

Figure 7: R_{SC} (approx. R_P) vs. efficiency under low illumination (filtered AM1.5 with intensity of 4.4W/m^2)

A further area of interest for the IPV practitioner is the impact of spectrum. It has been demonstrated in Figure 3 that amorphous Silicon sample efficiency was higher with fluorescent spectrum (up 14-34% at 2W/m^2) whilst the crystalline Silicon samples efficiency deteriorated (down 51-57% at 2W/m^2) compared with filtered AM1.5. It would be interesting to test other samples as well as corroborate the results with comparison of the spectral response. The latter was not pursued, as the selection of samples did not include a single cell sample (a pre-requisite for the spectral response equipment) for each technology.

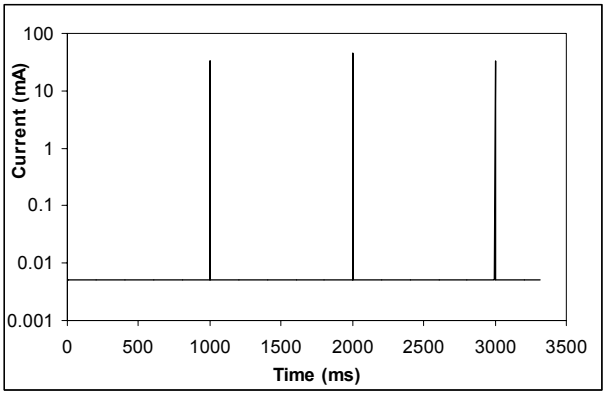

Figure 8: Typical charge consumption of datalogging or sensor device

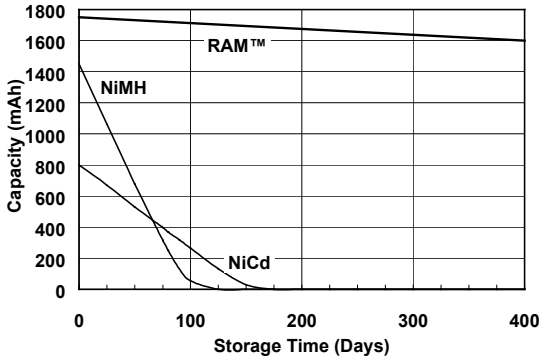

Figure 9: Secondary cell self-discharge technology comparison, courtesy of Battery Technologies Inc.

For those interested in developing IPV products, there are other important factors apart from the Photovoltaic design. Ideal products that can benefit from PV power perform datalogging and/or sensor functions. This is

because their functionality is only required in intermittent spikes separated by relatively long "rest" periods (e.g. a typical ratio of in-function to stand-by time of 1:1000) such as Figure 8.
The main charge consumption need is therefore the standby current, which unfortunately for many present IC designs can be of the order of mA rather than the μA typically produced indoors by PV. The development of ever more efficient micro-controller standby/sleep modes is important for PV penetration in indoor products.
Most IPV products require charge storage to allow use when E_{rad} is too low. A number of charge storage technologies are available, one of which (RAM^{TM}) is well adapted to IPV due to its low leakage current (see Figure 9).
Other aspects of design are also important including final appearance, intelligent integration of PV device and giving preference to solar cell orientations that are directed towards the E_{rad} sources.

CONCLUSIONS

At the beginning of this paper, the lack of comparable low intensity solar cell data was mentioned. Results for 21 samples representing 8 technologies tested under two spectra have been presented. Also the reasons why existing solar cell comparisons are not applicable for indoor PV (IPV) design have been presented. For example, absolute efficiency may vary markedly with intensity in the decades 1-100W/m2 (see Figure 2).
The lack of appropriate models has also been identified; a two parameter phenomenologically based model has been shown to correlate well to experimental results in the intensity range of interest for IPV design.
This paper has identified a number of issues important to IPV design and has provided results that may contribute to better resolving them.

ACKNOWLEDGEMENTS

W. Durisch (PSI, CH), G. Leyland, M-O. Hongler, F. Dusonchet (all 3 at EPFL, CH) and E. Meyer (University of Port Elizabeth, South Africa) are thanked for helpful discussion. We are grateful to C. Droz (University of Neuchatel, CH) for providing corrections.

REFERENCES

1. Software available for payment free download on 31.1.02 via http://radsite.lbl.gov/radiance/HOME.html
2. IEC-904-3, *IEC Standard* (1989) i.e. 1000W/m2 AM1.5 perpendicular to the cell surface at 25°C
3. Randall, J.F., Droz, C., Goetz, M., Shah, A. and Jacot, J., (2001) 17th EPVSECE, Munich
4. classified as in Green, M.A., Emery K., King D.L., Igari, S. and Warta W. (2002) *Prog. Photovolt: Res. Appl.* **10**, 55-61
5. e.g. average for all samples of (FF maximum – FF minimum) for range 8-100W/m2 is 2% for CdTe, 5% for a-Si and dye cells, 22% for poly-crystalline Silicon and 23% for mono-crystalline Silicon.
6. Sze S.M. (2001) In: *Semiconductor Devices: Physics and Technology*. Wiley, New York
7. Möller, H. J., *Semiconductors for Solar Cells* (1993) Artech House pp. 29 Equation 2.39
8. Green M., *Solar Cells Operating Principles, Technology and System Applications* (1982) University of New South Wales pp. 88
9. R^2 calculated automatically by Microsoft Excel^{TM}. For more details, see the Microsoft Excel^{TM} Help function.
10. Green M., *Solar Cells Operating Principles, Technology and System Applications* (1982) University of New South Wales pp. 96-97
11. Merten J., Voz C., Munoz A., Asensi J. M., Andreu J., *Solar Energy Materials & Solar Cells* **57** (1999) 153-165 pp. 159